# Supporting Information

## Construction of Z-scheme heterojunction interfacial charge transfer pathways in $ZnIn_2S_4$@NENU-5 for photocatalytic hydrogen evolution

Xu Kong[1,2,3], Kai Wang[1,2,3]*, Hai Yu[1,2,3], Zhiliang Jin[1,2,3]

*1. School of Chemistry and Chemical Engineering, North Minzu University, Yinchuan 750021, P.R.China*

*2. Ningxia Key Laboratory of Solar Chemical Conversion Technology, North Minzu University, Yinchuan 750021, P.R.China*

*3. Key Laboratory for Chemical Engineering and Technology, State Ethnic Affairs Commission, North Minzu University, Yinchuan 750021, P.R.China*

*Corresponding author: kaiwang@nun.edu.cn (K. Wang)

**AQE measurement:**

The apparent quantum efficiency (AQE) for the photocatalytic hydrogen evolution from the sample was measured under the irradiation of 300 W Xe lamps at various monochromatic wavelengths (450 nm, 475 nm, 500 nm, 520 nm, and 550 nm), the AQE was then calculated using the following equation:

$$AQE = \frac{2 \times \text{the number of evolved hydrogen molecules}}{\text{the number of incident photons}} \times 100\%$$

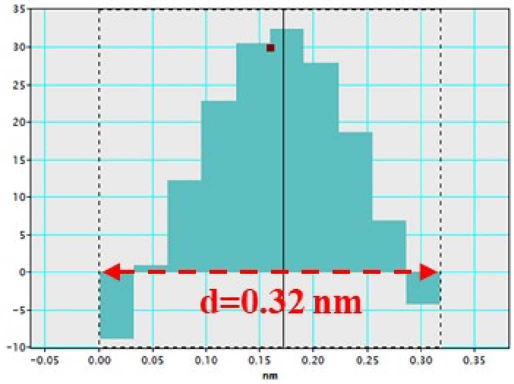


**Fig. S1.** Parameters of the lattice within the area of Fig. 2f

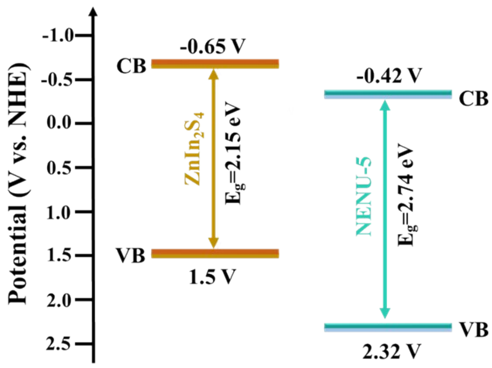


**Fig. S2.** band structures of NENU-5 NOs and $ZnIn_2S_4$ NFs.

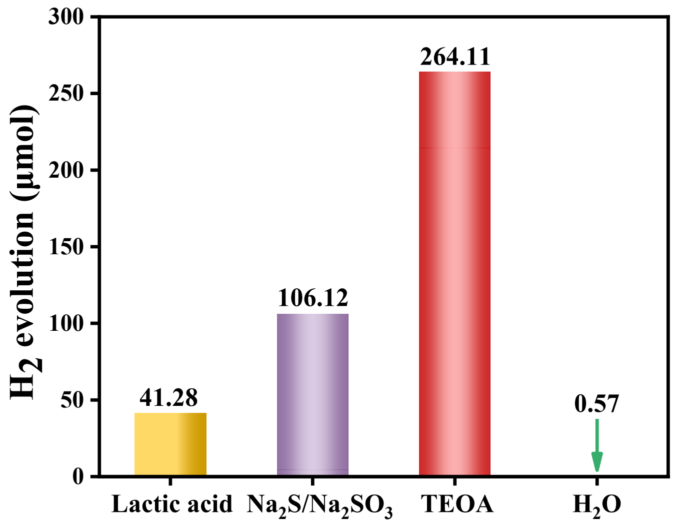


**Fig. S3.** $H_2$ evolution of the $ZnIn_2S_4$@10%NENU-5 in different sacrificial reagents.

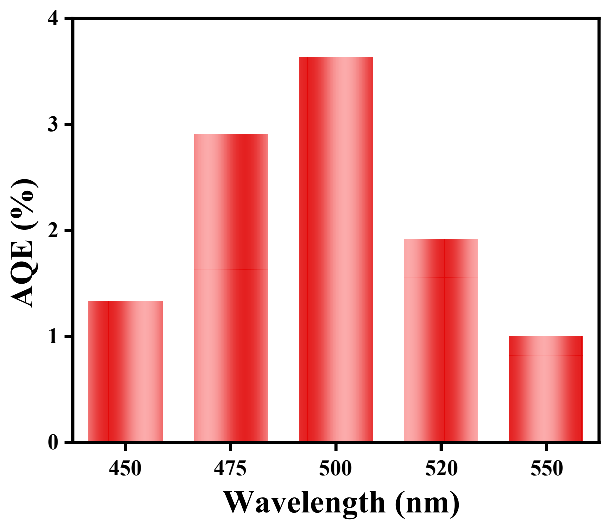


**Fig. S4.** Apparent quantum efficiency (AQE) of the $ZnIn_2S_4$@10%NENU-5.

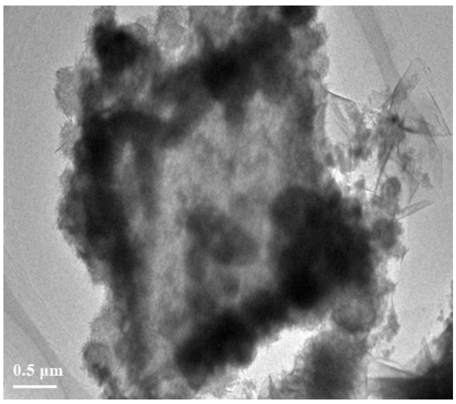


**Fig. S5.** TEM images of $ZnIn_2S_4$@NENU-5 heterostructures after photocatalytic reaction.

**Table S1.** Parameters of physical adsorption

| Samples | $S_{BET}$ ($m^2g^{-1}$) | Pore volume ($cm^3g^{-1}$) | Average pore size (nm) |
|---|---|---|---|
| NENU-5 NOs | 547.02 | 0.22 | 6.13 |
| $ZnIn_2S_4$ NFs | 65.29 | 0.23 | 12.29 |
| ZIS@10%NENU-5 | 101.39 | 0.34 | 11.96 |

**Table S2.** Comparison of photocatalytic hydrogen evolution rate of $ZnIn_2S_4$ based photocatalysts.

| Photocatalysts | Light sources | Sacrificia l reagent | AQE (%) @wavelength | Activity (μmol·$g^{-1}$ $h^{-1}$ ) | Ref. |
|---|---|---|---|---|---|
| $ZnIn_2S_4$@NENU-5 | 5 W LED | TEOA | 500 nm 3.64% | 5282.14 | This work |
| $ZnIn_2S_4/MoS_2$ | 150 W Xe lamp | $Na_2S/Na_2SO_3$ | 532 nm 0.19% | 200.1 | [S1] |
| $FeIn_2S_4$@$ZnIn_2S_4$ | 300 W Xe lamp | $Na_2S/Na_2SO_3$ | 420 nm 3.69% | 4210 | [S2] |
| $NiTiO_3/ZnIn_2S_4$ | 3X 30W LED | TEOA | 450 nm 4.39% | 4430 | [S3] |
| MIL-68(In)@$ZnIn_2S_4$ | 300 W Xe lamp | TEOA | 400 nm 0.70% | 9090 | [S4] |
| $MoO_2$/C@$ZnIn_2S_4$ | 300 W Xe lamp | TEOA | 400 nm 2.96% | 2357 | [S5] |
| $Ti_3C_2/ZnIn_2S_4$/CdS | 300 W Xe lamp | TEOA | 450 nm 3.42% | 8930 | [S6] |
| BP@$ZnIn_2S_4$ | 300 W Xe lamp | $Na_2S/Na_2SO_3$ | 450 nm 0.25% | 1278 | [S7] |
| $Ni_{1-x}Co_xSe_2$-C /$ZnIn_2S_4$ | 300 W Xe lamp | TEOA | 420 nm 2.32% | 5099 | [S8] |
| $ZnIn_2S_4$@$NH_2$-MIL-125(Ti) | 300 W Xe lamp | $Na_2S/Na_2SO_3$ | 420 nm 4.30% | 2204 | [S9] |

**Table S3.** Attenuation parameters of all samples.

| Sample | $\tau_1$ [ns] | $\tau_2$ [ns] | $\tau_3$ [ns] | $\tau_{ave}$ [ns] |
|---|---|---|---|---|
| NENU-5 NOs | 2.117 (11.80%) | 0.048 (83.74%) | 11.754(4.45%) | 0.057 |
| $ZnIn_2S_4$ NFs | 2.204(10.50%) | 13.137 (3.89%) | 0.056(85.61%) | 0.065 |
| ZIS@10%NENU-5 | 2.222(11.59%) | 0.083 (83.95%) | 12.849(4.46%) | 0.098 |

**References**

[S1] W. Pudkon, H. Bahruji, P. J. Miedziak, T. E. Davies, D. J. Morgan, S. Pattisson, S. Kaowphong and G. J. Hutchings, Enhanced visible-light-driven photocatalytic $H_2$ production and Cr(VI) reduction of a $ZnIn_2S_4/MoS_2$ heterojunction synthesized by the biomolecule-assisted microwave heating method, *Catal. Sci. Technol.*, 2020, **10**, 2838-2854.

[S2] Fan Q, Yan Z, Li J, et al. Interfacial-electric-field guiding design of a Type-I $FeIn_2S_4$@$ZnIn_2S_4$ heterojunction with ohmic-like charge transfer mechanism for highly efficient solar $H_2$ evolution, *Appl. Surf. Sci.*, 2024, **663**, 160206.

[S3] S. Dhingra, M. Sharma, V. Krishnan and C. Nagaraja, Design of noble metal-free $NiTiO_3/ZnIn_2S_4$ heterojunction photocatalyst for efficient visible-light-assisted production of $H_2$ and selective synthesis of 2, 5-Bis (hydroxymethyl) furan, *J. Colloid Interface Sci.*, 2022, **615**, 346-356.

[S4] M. Tan, C. Yu, H. Zeng, C. Liu, W. Dong, H. Meng, Y. Sua, L. Qiaoa, L. Gaoa, Q. Luc and Y. Bai, In situ fabrication of MIL-68(In)@$ZnIn_2S_4$ heterojunction for enhanced photocatalytic hydrogen production, *Nanoscale*, 2023, **15**, 2425-2434.

[S5] X. Zhang, H. Ye, Z. Zeng, K. Sa, J. Jia, Z. Yang and S. Xu, Chuang Han, Yujun Liang, Bridging the gap between metallic $MoO_2$ and $ZnIn_2S_4$ for enhanced photocatalytic $H_2$ production, *Sep. Purif. Technol.*, 2024, **347**, 127624.

[S6] J. Bai, W. Chen, R. Shen, Z. Jiang, P. Zhang, W. Liu and X. Li, Regulating interfacial morphology and charge-carrier utilization of $Ti_3C_2$ modified all-sulfide $CdS/ZnIn_2S_4$ S-scheme heterojunctions for effective photocatalytic $H_2$ evolution, *J. Mater. Sci. Technol.*, 2022, **112**, 85-95.

[S7] Q. Zhanga, J. Zhanga, L. Zhanga, M. Caoa, F. Yanga and W. L. Dai, Facile construction of flower-like black phosphorus nanosheet@$ZnIn_2S_4$ composite with highly efficient catalytic performance in hydrogen production, *Appl. Surf. Sci.*, 2020, **504**, 144366.

[S8] Y. Chao, P. Zhou, J. Lai, W. Zhang, H. Yang, S. Lu, H. Chen, K. Yin, M. Li, Lu Tao, C. Shang, M. Tong and S. Guo, $Ni_{1-x}Co_xSe_2$-C/$ZnIn_2S_4$ Hybrid Nanocages with Strong 2D/2D Hetero-Interface Interaction Enable Efficient $H_2$-Releasing

Photocatalysis, *Adv. Funct. Mater.*, 2021, **31**, 2100923.
[S9] H. Liu, J. Zhang and D. Ao, Construction of heterostructured $ZnIn_2S_4$@$NH_2$-MIL-125 (Ti) nanocomposites for visible-light-driven $H_2$ production, *Appl. Catal. B Environ. Energy*, 2018, **221**, 433-442.